Proceedings of the 2010 IEEE
International Conference on Information and Automation
June 20 - 23, Harbin, China

A Three-Dimensional Visual Localization System Based on Four Inexpensive Video Cameras

Wei Liu, Chao Hu and Qing He

Shenzhen Institutes of Advanced Technology, Chinese Academy of Sciences
Key Lab for Biomedical Informatics & Health Eng. CAS
Shenzhen Key Lab for Low-Cost Health, SIAT

wei.liu@sub.siat.ac.cn chao.hu@siat.ac.cn

Max Q.-H. Meng

IEEE Fellow

Chinese University of HongKong

max@ee.cuhk.edu.hk

***Abstract* - In order to achieve the goal of high accuracy and low cost in a visual localization system, we present a novel localization method based on four inexpensive video cameras. The method mainly consists of two parts: The "16-points interpolation algorithm" is proposed to enhance the accuracy of 2D coordinates of the detected target on the image plane. Another important aspect is that the Perpendicular Foot Method (PFM) is used to calculate the 3D coordinates of the target. Simulation and real experimental results show that the stability of image coordinates (x, y) is significantly improved by the "16-points interpolation algorithm", and the PFM algorithm is better than the traditional LSM (Least Square Method) algorithm. The localization accuracy of this system can reach 5mm, when the target is moved along with the y axes direction which is perpendicular to the optical axes of CCD cameras.**

Index Terms – Computer Vision, Localization, CCD Camera

I. INTRODUCTION

Multiple cameras system has been applied to a wide rage of important areas of computer vision. For example object modelling based on 2D images of multi-cameras [1,2], multi-cameras for panorama photography [3], high speed videography [4] and the object tracking in visual surveillance applications [5]-[7] are all the hot topics in the field of computer vision. One another interesting and challenging topic in the multi-cameras system is the three dimensional visual measurement. For example, Frank Cheng et al proposed a three dimensional binocular stereo vision system in industrial robot applications to enhance the robot flexibility and intelligence [8]. However, because there are only two cameras used in its system, the measurement result is not accurate enough. Paul Wade et al introduced a trinocular stereo vision system for robust and accurate 3D measurement of formed tube [9]. This three cameras system has better measurement accuracy than the two cameras system.

In order to realize the goal of high accuracy and low cost, we proposed a multi-cameras stereo visual localization method based on four inexpensive video surveillance cameras. Compared with the past stereo visual measuring systems, more cameras are used in our system to improve the localization accuracy. Moreover, these cameras are all inexpensive surveillance cameras with low image-quality and large distortion. Due to the increasing number of cameras, the topology of cameras distribution, the theoretical model and the localization algorithm are all different from the before. The simulation and real experiment show that four CCD cameras stereo visual localization system has good accuracy of localization.

In Section II, the hardware of the three-dimensional visual localization system base on four expensive CCD cameras is presented firstly, and then a simple color-based object recognition algorithm is used to detect the interested point in the image plane. But considering the low imaging quality of our system, the image coordinates of the detected target may not be accurate enough. So the image points of 16 consecutive frames of single video cameras are utilized to interpolate a fine coordinates which is called the "16-points interpolation algorithm". Given the extrinsic and intrinsic camera parameters, each image point defines a ray in three dimensional spaces, and in the absence of measurement errors, all rays from different cameras intersect in the same object point. But actually the four rays may not intersect in the same point due to the low-quality video cameras and other complicated reasons. The perpendicular foot method (PFM) for multi-cameras localization is proposed in the fifth part of Section II to solve this problem. A large number of experiments in Section III prove that our system has a good performance in object localization. Some discussion and conclusions are drawn in Section IV.

II. SYSTEM ARCHITECTURE

A. Hardware

Our 3D measurement system by multi-cameras is easy to be built up. It mainly consists of three parts: four low-quality video surveillance cameras, two two-channel video capture cards and other sets such that a chessboard for camera calibration and PC. Figure 1 shows the CCD sensor board in video camera, an optical lens and a video capture card in the system. The Sony ICX409AK CCD which is a low-end CCD image sensor suitable for PAL color video cameras is adopted to generate progressive video frame at 25 fps (frames per second). In addition, four inexpensive IR lenses with fixed focal length and large distortion are mounted on the head of cameras. Two of them are used to grab wider field of view with 4-mm focal length, while the other two lenses are with

978-1-4244-5704-5/10/$26.00 ©2010 IEEE

Fig. 1. The chief hardware used in the system

6-mm focal length. The V110 video capture card which is manufactured by Microview Corporation is a frame grabber for color video acquisition based on PCI bus. It features two CVBS input and one S-video input, and stable inception of the standard video signals from various video sources. Its resolution can be up to 768 × 576. The outstanding features of V110 are high price performance ratio and good compatibility. Two cards' price is less than 100 dollars. The cost of total sets mentioned above (exclude the PC) is about 200 dollars.

B. *Algorithms Flow Char*

In this section, the software flow chart of the 3D localization algorithm based on four video cameras will be introduced. First of all, the hardware interruptions of each camera are initialized. When one frame is captured completely in a camera, the hardware interruption will be trigged, and then the interruption service routine of this camera will be run. As shown in Figure 2, the methods described in the dash line rectangles are the mainly localization algorithms of our system, which can be summarized in four steps as follows:

1) Image Distortion Calibration: The "barrel distortion" exists in the four camera lenses in our system, which leads to image magnification decreases with distance from the optical axis. If the "barrel distortion" is not clear, the image coordinates (*u, v*) of the target (a ping pong ball in our experiment) calculated by the step *2)* and step *3)* will not be accurate.

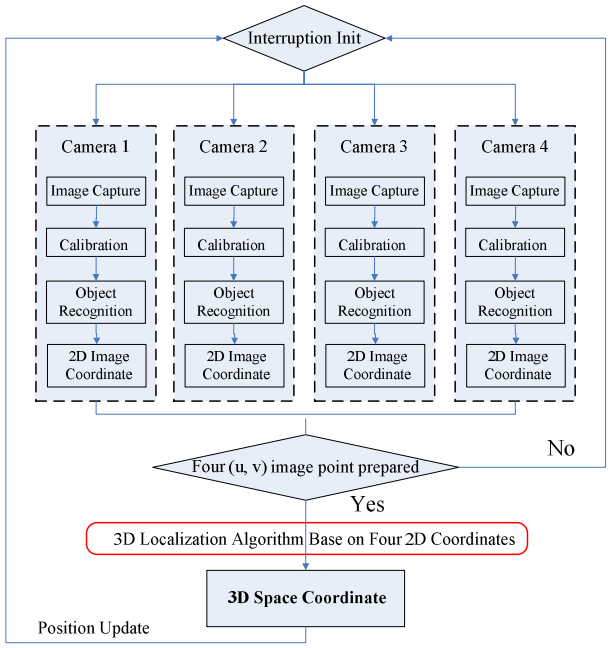

Fig. 2. The flow chart of the system

2) Object Recognition: The measured target in our experiment is an orange-color ping pong ball. The centre point of ping pong ball must be found in each video camera scene before calculating the 3D coordinates of the ping pong ball centre. Color-space model is used in the ping pong ball recognition algorithm to decide the image coordinates (*u, v*) of the ping pong ball.

3) 2D Image Coordinates Calculation: Due to different noises existing in the system such that the imaging noise and the illumination noise, the image coordinates (*u, v*) of the detected target in a single video camera may not be accurate enough. So the image points of 16 consecutive frames of single video cameras are utilized to interpolate a fine coordinates.

4) 3D Localization Algorithm: The "Least Square Method" (LSM) is used to estimate the best localization point in a traditional way. But the LSM algorithm has its limitation that is proven in the following experiment. A new 3D localization algorithm based on multiple image coordinates is presented in our system. "Perpendicular Foot Method" (PFM) is adopted to estimate the best point of the measured target.

C. *Camera Calibration*

In the machine vision field, camera calibration is a vital step in deciding the measuring accuracy. Because the influence of barrel distortion of lenses, the inaccuracy of focal length and principle point's position exist in our system, instinct parameters of cameras are needed to be determined before 3D measurement, which is given by

$$A = \begin{bmatrix} \alpha & \gamma & u_0 \\ 0 & \beta & v_0 \\ 0 & 0 & 0 \end{bmatrix}$$

with (u_0, v_0) the coordinates of the principle point, and the scale factors in image u and v axes, and the parameter describing the skewness of the two image axes.

Besides the intrinsic parameters of cameras, the extrinsic parameters — rotation matrix R and transition matrix T — are also needed to be initialized before 3D measuring. After building the camera coordinates system Oc-XcYcZc and the world coordinates system Ow-XwYwZw, the camera's position (*tx, ty, tz*) and rotation angle (, ,) in a fixed world coordinates system Ow-XwYwZw can be described as shown in Figure 3.

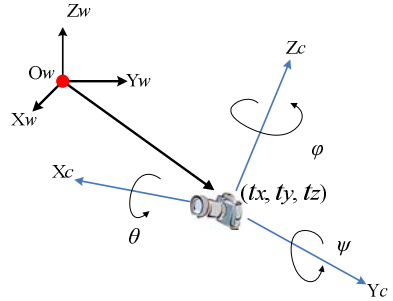

Fig. 3. The camera's position and angle in a world coordinates system

The coordinates (*tx, ty, tz*) represents the translation vector, The angles: , and denote the degree of rotation around x

axes, y axes and z axes respectively. The extinct parameters is given by

$$\boldsymbol{B} = \begin{bmatrix} r_{11} & r_{12} & r_{12} & tx \\ r_{21} & r_{22} & r_{23} & ty \\ r_{31} & r_{32} & r_{33} & tz \\ 0 & 0 & 0 & 1 \end{bmatrix} \begin{cases} r_{11} = \cos\psi\cos\phi \\ r_{12} = \sin\theta\sin\psi\cos\phi - \cos\theta\sin\phi \\ r_{13} = \cos\theta\sin\psi\cos\phi - \sin\theta\sin\phi \\ r_{21} = \cos\psi\sin\phi \\ r_{22} = \sin\theta\sin\psi\sin\phi + \cos\theta\cos\phi \\ r_{23} = \cos\theta\sin\psi\sin\phi - \sin\theta\cos\phi \\ r_{31} = \sin\psi \\ r_{32} = \sin\theta\cos\psi \\ r_{33} = \cos\theta\sin\psi \end{cases}$$

Both A and B can be acquired by the Zhang's method [10] in the following experiment.

D. Object Recognition and 2D coordinates Calculation

In our system, the measured target is a standard orange-color ping pong ball with 40-mm diameter. The projection of ping pong ball by any video camera is an orange-color circle. The target of object recognition is to find the orange-color ping pong ball and decide the coordinates of its centre point. Color-space model of the ping pong ball is firstly established: the vector [*Rp, Gp, Bp*] represents the color components of ping pong ball. It is the color components of current pixel to be selected. σ_r, σ_g and σ_b (σ_r=0.03, σ_g=0.08 and σ_b=0.09 in our system)denote the threshold of the three color component deviation. If the following inequality (1) is satisfied, the current pixel is flagged to be processed further.

$$\begin{cases} |R - R_p| \le \sigma_r \\ |G - G_p| \le \sigma_g \\ |B - B_p| \le \sigma_b \end{cases} \quad (1)$$

After scanning all pixels in the image, the gravity centre of all flagged pixels can be determined as the image point coordinates (*x, y*). But the coordinates (*x, y*) can not be utilized immediately, because many noises will cause the big variance and instability on it. Corresponding data of the raw coordinates (*x, y*) will be presented in the following experiment section. A 16-points interpolation algorithm is introduced in our system to remove those errors. Formula (2) describes a quadratic fitting curve equation, where computational result *F(t)* is the substitute for the current sample value. The parameter *t* can be selected from 1 to *n* — — the length of the interpolation window.

$$F(t) = w_1 t^2 + w_2 t + w_3 \quad (2)$$

The parameters w1, w2 and w3 are the coefficients of the quadratic curve, which can be calculated by LSM method as forum (3), with n the length of the interpolation window, *f(i)* the *i*th sample value in the interpolation window. In our system, the parameter *n* is 16. The *f(i)* can be substituted by the image coordinates *x* and *y* of the ball center separately in each camera.

$$\begin{pmatrix} w_1 \\ w_2 \\ w_3 \end{pmatrix} = \begin{pmatrix} \sum_{i=0}^{n} i^4 & \sum_{i=0}^{n} i^3 & \sum_{i=0}^{n} i^2 \\ \sum_{i=0}^{n} i^3 & \sum_{i=0}^{n} i^2 & \sum_{i=0}^{n} i \\ \sum_{i=0}^{n} i^2 & \sum_{i=0}^{n} i & \sum_{i=0}^{n} 1 \end{pmatrix}^{-1} \begin{pmatrix} \sum_{i=0}^{n} f(i) i^2 \\ \sum_{i=0}^{n} f(i) i \\ \sum_{i=0}^{n} f(i) \end{pmatrix} \quad (3)$$

E. Localization Algorithm

In this section, we firstly discuss the ideal case of classical projection theory. In the ideal case, all polar lines of each camera intersect in the same point, i.e. the object point. But in the real condition, the polar lines of each camera may not cross at the same point. A new method call PFM is proposed to calculate the object's 3D coordinates in the later conditions.

1) Ideal Cases:

Here, take two cameras projection for example. As shown in Figure 4, according the geometrical optics, two rays of different cameras cross at the object point (*Xw, Yw, Zw*). In classical projection theory, the relationship between object point and image point is given by

$$\begin{cases} \begin{bmatrix} x \\ y \\ 1 \end{bmatrix} = \frac{1}{z_c} \begin{bmatrix} f & 0 & 0 & 0 \\ 0 & f & 0 & 0 \\ 0 & 0 & 1 & 0 \end{bmatrix} \begin{bmatrix} R & t \\ 0 & 1 \end{bmatrix} \begin{bmatrix} X_w \\ Y_w \\ Z_w \\ 1 \end{bmatrix} \\ z_c = X_w r_{31} + Y_w r_{32} + Z_w r_{33} + t_z \end{cases} \quad (4)$$

with (X*w*, Y*w*, Z*w*) the world coordinate, (*x*, *y*) the image coordinates, R the rotation matrix, t the translation vector and f the focal length, r_{31}, r_{32}, r_{33}, t_z the component elements of rotation matrix R and translation vector t. Theoretically, if the two image points coordinates (*x*, *y*) of different cameras are known, the object's 3D coordinates could be calculated by forum (5)

$$\begin{cases} \begin{bmatrix} Xw \\ Yw \\ Zw \end{bmatrix} = k \begin{bmatrix} x_0 \\ y_0 \\ f_0 \end{bmatrix} + \begin{bmatrix} \Delta x \\ \Delta y \\ \Delta z \end{bmatrix} \\ [x_0, y_0, z_0]^T = R^T [x, y, f] \\ [\Delta x, \Delta y, \Delta z]^T = -R^T t \\ k = z / f \end{cases} \quad (5)$$

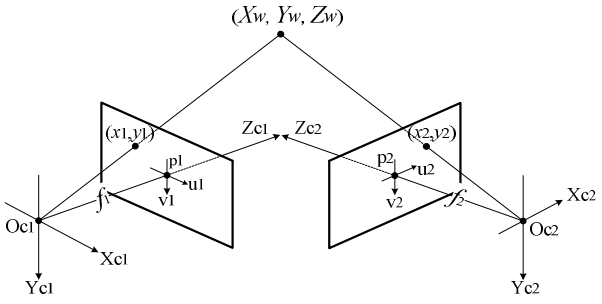

Fig. 4. The ideal case of classical projective theory

2) Real Cases:

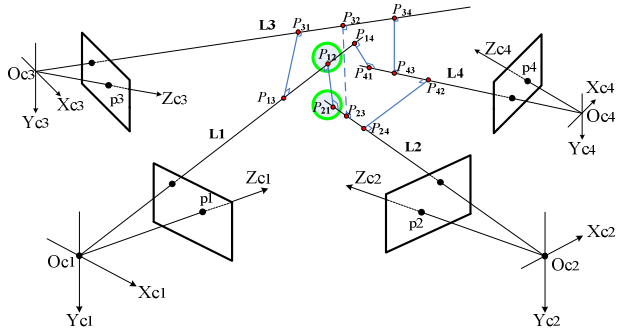

Fig. 5. The real case of four cameras projection

In the real conditions, the "polar lines" often constitute a group of non-coplanar lines as shown in Figure 5, any two lines of L1, L2, L3 and L4 do not cross at the same point. In post researches, the "Least Square Method" is used to estimate the best position of the target based on these non-coplanar "polar lines". In this paper, a novel effective method call "Perpendicular Foot Method" (PFM) is proposed.

As shown in Figure 5, the four "polar lines" L1, L2, L3 and L4 are a group of non-coplanar lines with six common vertical lines and twelve perpendicular points denoted as P_{ij},

Take the L1 and L2 "polar lines" for example, the two perpendicular points is marked with two bold circles in the Figure 5. Let

$$\begin{aligned} L_1 &= r_1 + rv_1 \\ L_2 &= r_2 + sv_2 \end{aligned} \tag{6}$$

with v_1 and v_2 the unit direction vector of "polar lines", r_1 and r_2 the translation vector, and r and s the parameters to be solved by the following formula:

$$\begin{cases} a = \prec v_1, v_1 \succ \\ b = \prec v_2, v_2 \succ \\ c = \prec v_1, v_2 \succ \\ d = \prec v_1, r_1 - r_2 \succ \\ e = \prec v_2, r_1 - r_2 \succ \end{cases} \Rightarrow \begin{cases} r = \dfrac{cd+ae}{c^2-ab} \\ s = \dfrac{bd+ce}{c^2-ab} \end{cases} \Rightarrow \begin{cases} P_{12} = r_1 + rv_1 \\ P_{21} = r_2 + sv_2 \end{cases} \tag{7}$$

According to formula (7), the coordinates of the two perpendicular points of the polar lines L1 and L2 can be calculated. We can use the mean position of P_{12} and P_{21} to denote the object point coordinates.

If k cameras exist in a system, the coordinates of object point in the world coordinates system can be given by

$$P = \frac{1}{k(k-1)} \sum_{1 \le i < j \le k} P_{ij} \tag{8}$$

with P_{ij} the perpendicular points of all "polar lines". The intermediate result P_{ij} can be calculated by the forum (7) by any two "polar lines" in Figure 5. The optimal solution of the object 3D coordinates can be defined as the mean position of all perpendicular points. The computational complexity of the PFM algorithm is quiet low, and the experiment of this PFM algorithm shows good results, which will be given in the following section.

III. Experimental Results

A. Simulation Experiments of Localization Algorithm

The accuracy of rotation matrix ***R*** and translation vector ***t***, the two-dimensional image coordinates **(*x, y*)** and the error of focal length ***f*** of CCD cameras are the four major factors in the localization accuracy of the system. In each type of these four factors, we compare the LSM method with the PFM method based on 1,000 group data with uniform-distribution noises. It is notable that the "binocular vs. four-view" comparisons have been done in TABLE II – TABLE V. The extinct parameters and focal length *f* in this simulation experiment is in the TABLE I. The centre of the world coordinates system is located at the centre of the camera 1 and camera 2.

TABLE I
The Extinct Parameters of Four CCD Cameras In Real Experiments

	(rad)	(rad)	(rad)	*tx*(mm)	*ty*(mm)	*tz*(mm)	*f*(mm)
Cam1	0	0	0	-200	0	0	4
Cam2	0	0	0	200	0	0	4
Cam3	0	- π /4	0	-500	0	500	6
Cam4	0	π /4	0	500	-0	500	6

TABLE II
Errors of Rotation Matrix *R*

	Average errors (mm) / Standard deviations (mm)		
Input errors(a)	Binocular (LSM)	Four-view (LSM)	Four-view (PFM)
± 0.5degree	5.21mm / 2.63mm	1.69mm / 0.63mm	1.56mm / 0.59mm
± 1 degree	10.2mm / 5.94mm	3.57mm / 1.28mm	3.25mm / 1.25mm
± 2 degree	21.1mm / 11.9mm	7.16mm / 2.63mm	6.56mm / 2.62mm
± 3 degree	31.1mm / 18.1mm	10.7mm / 3.90mm	9.73mm / 3.85mm

The "Input errors" are the noise added onto the rotation matrix *R*. These noises obey the uniform distribution *U*(-a, a).

TABLE III
Errors of Translation Vector *T*

	Average errors (mm) / Standard deviations (mm)		
Input errors(a)	Binocular (LSM)	Four-view (LSM)	Four-view (PFM)
± 0.5mm	0.94mm / 0.54mm	0.40mm / 0.14mm	0.33mm / 0.14mm
± 1.0mm	1.83mm / 1.12mm	0.81mm / 0.29mm	0.67mm / 0.28mm
± 2.0mm	3.72mm / 2.18mm	1.59mm / 0.59mm	1.35mm / 0.57mm
± 4.0mm	7.49mm / 4.26mm	3.25mm / 1.17mm	2.72mm / 1.15mm
± 10.0mm	19.1mm / 11.3mm	7.97mm / 2.98mm	6.86mm / 2.95mm

The "Input errors" are the noise added onto the translation vector *t*. These noises obey the uniform distribution *U*(-a, a).

TABLE IV
Errors of Image Coordinates (*X, Y*)

	Average errors (mm) / Standard deviations (mm)		
Input errors(a)	Binocular (LSM)	Four-view (LSM)	Four-view (PFM)
± 1 pixels	1.80mm / 1.04mm	0.63mm / 0.23mm	0.57mm / 0.23mm
± 2 pixels	3.57mm / 2.09mm	1.25mm / 0.46mm	1.15mm / 0.44mm
± 4 pixels	7.15mm / 4.13mm	2.52mm / 0.93mm	2.31mm / 0.93mm
± 8 pixels	14.4mm / 8.44mm	5.19mm / 1.86mm	4.70mm / 1.81mm

The "Input errors" are the noise added onto the image coordinates (*x, y*). These noises obey the uniform distribution *U*(-a, a).

TABLE V
ERRORS OF FOCAL LENGTH *F*

	Average errors (mm) / Standard deviations (mm)		
Input errors(a)	Binocular (LSM)	Four-view (LSM)	Four-view (PFM)
± 0.5%	1.73mm / 1.08mm	0.42mm / 0.33mm	0.25mm / 0.16mm
± 1%	3.65mm / 2.20mm	0.85mm / 0.64mm	0.48mm / 0.32mm
± 2%	6.93mm / 4.41mm	1.68mm / 1.31mm	1.03mm / 0.66mm
± 4%	14.3mm / 8.59mm	3.37mm / 2.69mm	1.94mm / 1.32mm

The "Input errors" are the noise added onto the focal length *f*. These noises obey the uniform distribution *U*(-a, a).

According to the tables above, we could find that the localization accuracy in PFM algorithm is preferred than the traditional LSM algorithm.

B. Real Data Experiments

In the real experiment, four CCD video cameras are located in front of the ping pong ball away from about 1.5 meters as shown in Figure 6. Because the No.3 and No.4 CCD video cameras are nearer to the measured target, wider range of view are needed to cover the whole scenes of different positions of ping pong ball, hence the focal length of these two cameras are 4 mm, while the No.1 and No.2 CCD video cameras are with 6-mm focal length lenses.

As shown in Figure 6, without loss of generality, we chose one fixed point "**O**" on the table to build up the world coordinates system in the real experiment. The x axes is rightward along with the table plane, while the y axes is perpendicular to the table plane, and the z axes is inward along with the table plane. The standard 3D coordinates of the ball centre can be measured by rules. Figure 7 shows the software programmed for four CCD cameras system 3D measurement

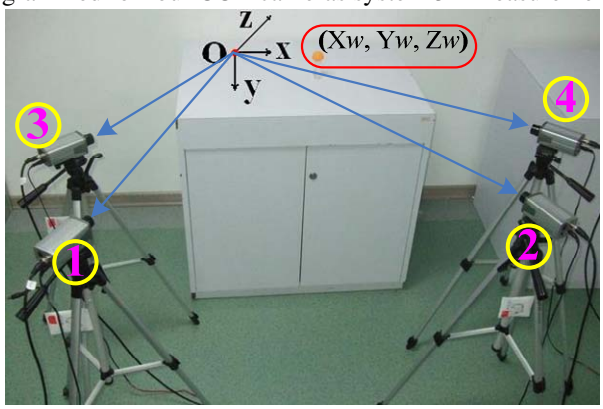

Fig. 6. The real experiment scene

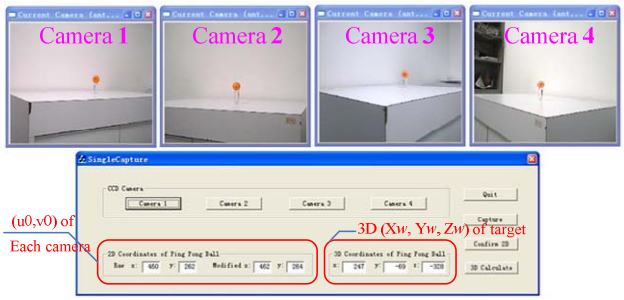

Fig. 7. The user interface of software in the system

The extinct parameters of these four CCD cameras in the real experiment are shown in TABLE VI, and the instinct parameters of these four CCD cameras are shown in TABLE VII. They are all calculated by Zhang's method in the current system.

TABLE VI
THE EXTINCT PARAMETERS OF FOUR CCD CAMERAS IN REAL EXPERIMENTS

	(rad)	(rad)	(rad)	*tx*(mm)	*ty*(mm)	*tz*(mm)
Cam1	0	0.541	0	-428	-60	-1054
Cam2	0.004	-0.349	0	590	-65	-1035
Cam3	0	0.838	0.002	-479	-60	-690
Cam4	0.001	0.794	0	730	-65	693

TABLE VII
THE INSTINCT PARAMETERS OF FOUR CCD CAMERAS IN REAL EXPERIMENTS

	(mm)	*(mm)*	*(mm)*	u_o	v_o
Cam1	6.76	6.76	0	316	298
Cam2	6.48	6.48	0	456	286
Cam3	5.07	5.07	0	478	288
Cam4	4.79	4.79	0	344	299

Figure 8 illustrates the 2D image coordinates (*x, y*) distribution of the ball centre, when the ball is located at a fixed position. We can easily find that the distribution of coordinates x and y after interpolations are more centralized than those before interpolations.

TABLE VIII gives the comparison of standard deviation of coordinates (*x, y*). It is demonstrated that the "16-points interpolation algorithm" is effective for stabilizing the image coordinates of measured target.

TABLE VIII
THE STANDARD DEVIATION OF MEASURED VALUE (*X, Y*)

	before Interpolation	after interpolation
x coordinates	0.8659 mm	0.3277 mm
y coordinates	2.0531 mm	0.7481 mm

After getting the image coordinates (*x, y*) of all cameras, 3D coordinates can be calculated by the PFM mentioned before. The experimental data are fitted surfaces in Figure 9, Figure 10 and Figure 11, when the ball moved along with three planes: x=100, y=-29 and z=-200 respectively. The fluctuant surfaces in these three figures represent the measured values, while the horizontal planes are the standard values.

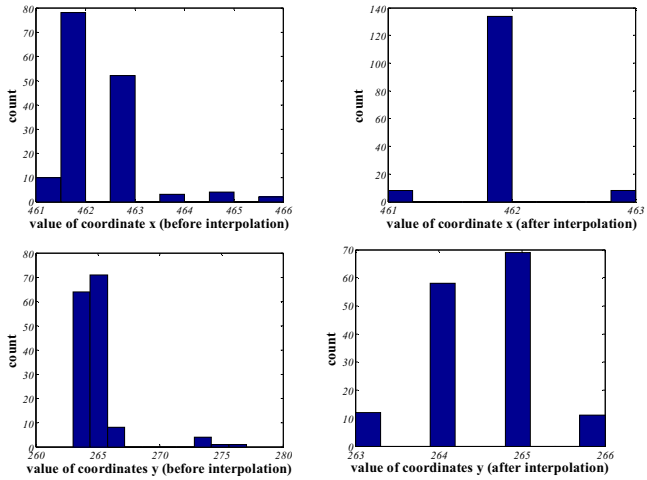

Fig. 8. The user interface of software in the system

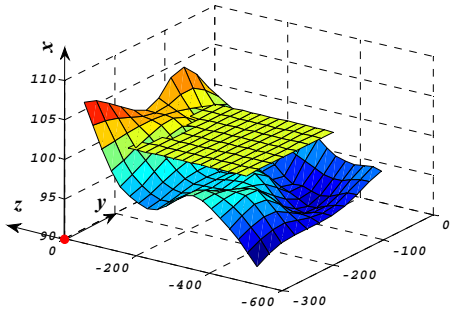

Fig. 9. The x = 100 plane experimental results

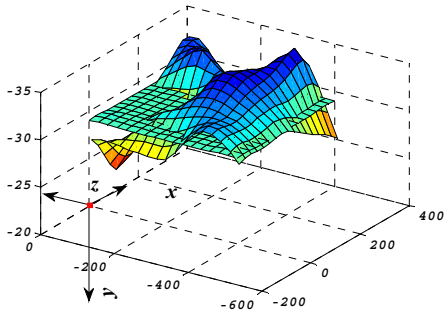

Fig. 10. The y = -29 experimental results

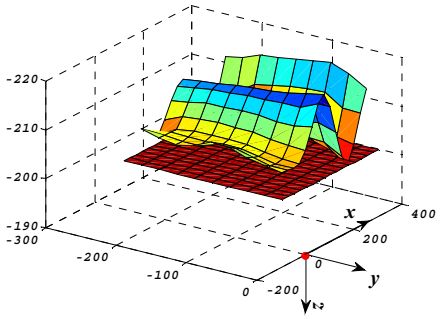

Fig. 11. The z = -200 experimental results

IV. Discussion And Conclusion

From the simulation experiments of localization algorithm in section III, We can find that the accuracy of the PFM algorithm is better than that of the LSM algorithm. Another conclusion is that the localization accuracy of four CCD cameras system is significantly superior to that of the binocular visual system, based on the four groups of contrast experiment.

From the real experiments in section III, we can find that the accuracy of image coordinates (*x, y*) can be improved by the interpolation algorithm. The localization errors is less than 5mm, when the ping pong ball moved along with the plane "y = -29". This y-direction localization accuracy is better than the other two cases, because the y axes is perpendicular to the optical axes of video cameras.

In order to enhance the x-axes direction's and the z-axes direction's localization accuracy of multi-cameras system, more cameras should be located at the directions which are perpendicular to the x-axes direction and the z-axes direction. This is a problem about topological structures of CCD cameras in visual localization system, which will be studied further in the future. In addition, from the simulation experiment, we can find that the rotation matrix, the translation vector and the focal length have effect on the localization accuracy. Hence, higher accuracy camera calibration method should be investigated to improve the accuracy of the instinct and extinct parameters of Cameras in future work.

References

[1] Zheng Shunyi, Wang Ruirui, Chen Changjun and Zhang Zuxun, "3D measurement and modeling based on stereo-camera," The International Archives of the Photogrammetry, Remote Sensing and Spatial Information Sciences, vol. XXXVII. Part B5. Beijing 2008.

[2] Soon-Yong Park and Murali Subbarao, "A multiview 3D modeling system based on stereo vision techniques," *Machine Vision and Applications*, vol. 16, No. 3, May 2005.

[3] 100 cameras array Tokyo, Japan 2006: http://www.virtualcamera.com/

[4] Bennett Wilburn, Neel Joshi and Vaibhav Vaish, "High speed video using a dense camera array," *Proc. CVPR 2004,* Washington, DC June, 2004.

[5] David Thirde and Mark Borg, "Multi-camera tracking for visual surveillance applications," *Computer Vision Winter Workshop 2006.* Czech Republic, February 6–8, 2006.

[6] John Krumm, Steve Harris and Brian Meyers, "Multi-camera multi-person tracking for easyliving," *Third IEEE International Workshop on Visual Surveillance*, July 1, 2000, Dublin, Ireland.

[7] Fleuret, F. Berclaz, J. Lengagne, R. and Fua, P, "Multi-camera people tracking with a probabilistic occupancy map," IEEE Transactions on Pattern Analysis and Machine Intelligence, pp. 267-282, June, 2007.

[8] Frank Cheng and Xiaoting Chen, "Integration of 3D Stereo Vision Measurements," *Proceedings of The 2008 IAJC-IJME International Conference,* Nov. 17-19, 2008, Nashville, TN.

[9] Paul Wade, David Moran, Jim Graham and C. Brook Jackson, "Robust and Accurate 3D Measurement of Formed Tube Using Trinocular Stereo Vision," *Electronic Proceedings of the 8th British Machine Vision Conference*, 1997, Essex, England

[10] Zhengyou Zhang, "A Flexible New Technique for Camera Calibration," IEEE Transactions on Pattern Analysis and Machine Intelligence, vol. 22, pp. 1330-1334, Nov 2000.